arXiv:hep-ph/0012003v1 1 Dec 2000

Study of $\Lambda_b \to \Lambda\ \nu\ \bar{\nu}$ with Polarized Baryons

Chuan-Hung Chen[a] **and C. Q. Geng**[b]

[a]*Department of Physics, National Cheng Kung University*
Tainan, Taiwan, Republic of China

[b]*Department of Physics, National Tsing Hua University*
Hsinchu, Taiwan, Republic of China

Abstract

We investigate the decay of $\Lambda_b \to \Lambda\ \nu\ \bar{\nu}$ with the polarized baryons of Λ_b and Λ. With the most general hadronic form factors, we first study the decay branching ratio and then derive the longitudinal, normal and transverse polarizations of Λ in terms of the spin unit vectors of Λ_b and Λ and the momentum of Λ. A polarization of Λ_b is also discussed.

1 Introduction

Recently, some of the interest in flavor physics has been focused in the rare decays related to $b \to sl\ \bar{l}$ induced by the flavor changing neutral current (FCNC) due to the CLEO measurement of the radiative $b \to s\gamma$ decay [1]. In the standard model, these rare decays occur at loop level and provide us with information on the parameters of the Cabibbo-Kobayashi-Maskawa (CKM) matrix elements [2] as well as various hadronic form factors. The corresponding rare decays of heavy hadrons such as $\Lambda_b \to \Lambda l^+ l^-$ have been studied in the literature [3, 4].

In this paper, we investigate the decay of $\Lambda_b \to \Lambda\ \nu\ \bar{\nu}$ with the polarized baryons of Λ_b and Λ. To study the decay, we shall use the most general hadronic form factors for the $\Lambda_b \to \Lambda$ transition. It is clear that this decay is free of long distance uncertainty like other di-neutrino decays of mesons [5]. However, there are many form factors when one evaluates the hadronic matrix elements between Λ_b and Λ, which are hard to be calculated since they are related to the non-perturbative effect of QCD. It is known that for heavy particle decays, the heavy quark effective theory (HQET) could reduce the number of form factors and supply the information with respect to their relative size. In our numerical calculations, we shall consider the cases with and without HQET. In our discussions of the decay branching ratio and the polarizations of Λ and Λ_b, we shall study the standard model and new physics such as those with right-handed hadronic currents.

The paper is organized as follows. In Sec. 2, we study the effective Hamiltonian for the di-neutrino decay of $\Lambda_b \to \Lambda\nu\bar{\nu}$ and form factors in the $\Lambda_b \to \Lambda$ transition. In Sec. 3, we derive the general forms of the differential decay rate and the longitudinal, normal and transverse polarizations of Λ. A polarization of Λ_b is also discussed. In Sec. 4, we give the numerical analysis. We present our conclusions in Sec. 5.

2 Effective Hamiltonian and Form factors

We start by writing the effective Hamiltonian for the inclusive process of $b \to s\nu\bar{\nu}$ as

$$\mathcal{H}\left(b \to s\ \nu\ \bar{\nu}\right) = \left[C_L\ \bar{s}\ \gamma_\mu\ P_L b + C_R\ \bar{s}\ \gamma_\mu\ P_R b\right] \bar{\nu}\ \gamma^\mu P_L \nu\,, \tag{1}$$

with $P_{L(R)} = \left(1 \mp \gamma_5\right)/2$, where we have assumed that the theories contain only $V - A$ and $V \pm A$-type interactions for the lepton and quark sectors, respectively. This can be justified if there is no contribution to the decay from right-handed neutrinos. Moreover, since the neutrino masses are very small, we expect that in our study only $V - A$-type of interactions for the lepton sector is important. In Eq. (1), $C_{L,R}$ are defined by

$$\begin{aligned} C_L &= C^{SM}\left(1 + \delta_L\right)\,, \\ C_R &= C^{SM}\delta_R\,, \\ C^{SM} &= \frac{G_F}{\sqrt{2}}\frac{\alpha_{em}}{\pi}\frac{2}{\sin^2\theta_w}V_{tb}V_{ts}^* X\left(x_t\right)\,, \end{aligned} \tag{2}$$

with

$$X\left(x_t\right) = \eta_{QCD}\frac{x_t}{8}\left[\frac{x_t + 2}{x_t - 1} + \frac{3x_t - 6}{\left(x_t - 1\right)^2}\ln x_t\right]\,, \tag{3}$$

where C^{SM} stands for the contribution from the standard model, $\delta_{L,R}$ denote the effects from new physics, $x_t = m_t^2/M_W^2$, and $\eta_{QCD} = 0.985$ is the QCD correction [6]. In the standard model, one has that $\delta_{L,R} = 0$. The constraints on $\delta_{L,R}$ will be discussed in Sec. 4. For calculating exclusive decays such as $\Lambda_b \to \Lambda\ \nu\ \bar{\nu}$, one has to evaluate the hadronic matrix element of the $\Lambda_b \to \Lambda$ transition. In general, one can express the vector and axial vector currents for the transition as

$$\begin{aligned} \langle\Lambda|\,\bar{s}\ \gamma_\mu\ b\,|\Lambda_b\rangle &= f_1\bar{u}_\Lambda\gamma_\mu u_{\Lambda_b} + if_2\bar{u}_\Lambda\sigma_{\mu\nu}\ q^\nu u_{\Lambda_b} + f_3 q_\mu \bar{u}_\Lambda u_{\Lambda_b}, \\ \langle\Lambda|\,\bar{s}\ \gamma_\mu\gamma_5\ b\,|\Lambda_b\rangle &= g_1\bar{u}_\Lambda\gamma_\mu\gamma_5 u_{\Lambda_b} + ig_2\bar{u}_\Lambda\sigma_{\mu\nu}\ q^\nu\gamma_5 u_{\Lambda_b} + g_3 q_\mu \bar{u}_\Lambda\gamma_5 u_{\Lambda_b}\,, \end{aligned} \tag{4}$$

where f_i and g_i $(i = 1, 2, 3)$ are the form factors and q is the momentum difference of the baryons, *i.e.*, $q = p_{\Lambda_b} - p_\Lambda$. It is clear that the terms corresponding to f_3 and g_3 have no contribution to the di-neutrinos decays for the massless neutrino case in the standard model, while that for the massive neutrinos, the effect is negligible. Therefore, we shall consider only the four independent form factors of $f_{1,2}$ and $g_{1,2}$ in Eq. (4). From Eqs. (1) and (4), we obtain the general form of the transition matrix element for $\Lambda_b \to \Lambda\nu\bar{\nu}$ as

$$\mathcal{M} = (F_1\bar{u}_\Lambda\gamma_\mu u_{\Lambda_b} + G_1\bar{u}_\Lambda\gamma_\mu\gamma_5 u_{\Lambda_b} + F_2\bar{u}_\Lambda\ \not{q}\gamma_\mu u_{\Lambda_b} + G_2\bar{u}_\Lambda\ \not{q}\gamma_\mu\gamma_5 u_{\Lambda_b}\ )\bar{\nu}\ \gamma^\mu P_L \nu, \tag{5}$$

where

$$F_i = \frac{C_R + C_L}{2} f_i\,, \quad G_i = \frac{C_R - C_L}{2} g_i\,, \quad (i = 1, 2)\,. \tag{6}$$

In HQET, the matrix elements in Eq. (4) can be simplified. Explicitly, from Ref. [9], one has that

$$\langle\Lambda|\,\bar{s}\ \Gamma\ b\,|\Lambda_b\rangle = \bar{u}_\Lambda\,(\mathcal{F}_1 + \not{v}\mathcal{F}_2)\,\Gamma u_{\Lambda_b}\,, \tag{7}$$

where Γ denotes the possible Dirac matrix and $v = P_{\Lambda_b}/M_{\Lambda_b}$ is the four-velocity of Λ_b. Comparing Eq. (7) with Eq. (4), we get

$$\begin{aligned} f_1 &= g_1 = \mathcal{F}_1 + \sqrt{r}\mathcal{F}_2, \\ f_2 &= g_2 = \frac{1}{M_{\Lambda_b}}\mathcal{F}_2, \end{aligned} \tag{8}$$

where $r = M_\Lambda^2/M_{\Lambda_b}^2$. Clearly, based on HQET, the form factors corresponding to the vector current are the same as that to the axial vector one, and the parts of the electric and magnetic moment are suppressed by the mass of the heavy particle. Therefore, there are only two independent form factors $\mathcal{F}_{1,2}$ and the form factors of the hadronic vector and axial vector currents are larger than that of the hadronic electric and magnetic currents in HQET.

3 Differential decay rate and Polarizations

To study the polarized baryon ($B = \Lambda_b$ or Λ), we write the four-spin vector of the baryon as

$$s_B^0 = \frac{\vec{p}_B \cdot \hat{\xi}_B}{M_B}, \qquad \vec{s}_B = \hat{\xi}_B + \frac{s_B^0}{E_B + M_B}\vec{p}_B\,, \tag{9}$$

where p_B is the momentum of B and $\hat{\xi}_B$ is the unit vector along the baryon spin in its rest frame.

In the Λ_b rest frame, we choose the unit vectors along the longitudinal, normal, transverse components of the Λ polarization as $\hat{e}_i$ $(i = L, N, T)$, defined by

$$\begin{aligned}
\hat{e}_L &= \frac{\vec{p}_\Lambda}{|\vec{p}_\Lambda|}\,, \\
\hat{e}_N &= \hat{e}_L \times \left(\hat{\xi}_{\Lambda_b} \times \hat{e}_L\right)\,, \\
\hat{e}_T &= \hat{\xi}_{\Lambda_b} \times \hat{e}_L\,,
\end{aligned} \tag{10}$$

respectively, where $\vec{p}_\Lambda$ is the momentum of Λ.

The partial decay rate for $\Lambda_b(p_{\Lambda_b}, s_{\Lambda_b}) \to \Lambda(p_\Lambda, s_\Lambda)\nu(p_1)\bar{\nu}(p_2)$ is given by

$$\begin{aligned}
d\Gamma &= \frac{1}{4M_{\Lambda_b}}\mathcal{M}\mathcal{M}^\dagger d\Phi\,, \\
d\Phi &= (2\pi)^4\,\delta^4\left(p_{\Lambda_b} - p_\Lambda - p_1 - p_2\right)\frac{d^3p_\Lambda}{(2\pi)^3\,2E_\Lambda}\frac{d^3p_1}{(2\pi)^3\,2E_1}\frac{d^3p_2}{(2\pi)^3\,2E_2}\,.
\end{aligned} \tag{11}$$

In the Λ_b rest frame, by integrating the phase space of ν and $\bar{\nu}$, from Eqs. (5) and (11) the partial decay rate in terms of the energy and polarizations of Λ is then given by

$$d\Gamma = \frac{1}{4}\left[1 + \frac{I_2}{I_1}\hat{e}_L \cdot \hat{\xi}_{\Lambda_b}\right]\left[1 + \vec{P}_\Lambda \cdot \hat{\xi}_\Lambda\right] d\Gamma^0\,, \tag{12}$$

with

$$d\Gamma^0 = 3\frac{G_F^2\alpha_{em}^2\,|V_{tb}V_{ts}^*|^2}{384\pi^6 M_{\Lambda_b}}\sqrt{E_\Lambda^2 - M_\Lambda^2}\;I_1\;dE_\Lambda\;d\Omega_\Lambda \tag{13}$$

and

$$\vec{P}_\Lambda = \frac{1}{1 + \frac{I_2}{I_1}\hat{e}_L \cdot \hat{\xi}_{\Lambda_b}}\left[\left(\frac{I_3}{I_1} + \frac{I_4}{I_1}\hat{e}_L \cdot \hat{\xi}_{\Lambda_b}\right)\hat{e}_L + \frac{I_5}{I_1}\hat{e}_N + \frac{I_6}{I_1}\hat{e}_T\right]\,, \tag{14}$$

where the factor 3 in Eq. (13) represents three families of neutrinos and I_i are defined by

$$\begin{aligned}
I_1 &= \left(|F_1|^2 + |G_1|^2\right)\left(q^2 p_{\Lambda_b} \cdot p_\Lambda + 2p_{\Lambda_b} \cdot q p_\Lambda \cdot q\right) + 3\left(|F_1|^2 - |G_1|^2\right) M_{\Lambda_b} M_\Lambda q^2 \\
&\quad - \left(|F_2|^2 + |G_2|^2\right)\left(q^4 p_{\Lambda_b} \cdot p_\Lambda - 4q^2 p_{\Lambda_b} \cdot q p_\Lambda \cdot q\right) - 3\left(|F_2|^2 - |G_2|^2\right) M_{\Lambda_b} M_\Lambda q^4 \\
&\quad - 6M_{\Lambda_b} q^2 p_\Lambda \cdot q\left(\mathrm{Re}\,F_2F_1^* - \mathrm{Re}\,G_2G_1^*\right) + 6M_\Lambda q^2 p_{\Lambda_b} \cdot q\left(\mathrm{Re}\,F_2F_1^* + \mathrm{Re}\,G_2G_1^*\right)\,,
\end{aligned} \tag{15}$$

$$\begin{aligned}
I_2 &= -2\,\mathrm{Re}\,F_1G_1^* M_{\Lambda_b}\left(q^2 - 2p_\Lambda \cdot q\right)\sqrt{E_\Lambda^2 - M_\Lambda^2} + 2M_{\Lambda_b} q^2\sqrt{E_\Lambda^2 - M_\Lambda^2}\,\times \\
&\quad \left[\mathrm{Re}\,F_2G_1^*\left(M_{\Lambda_b} + 3M_\Lambda\right) - \mathrm{Re}\,F_1G_2^*\left(M_{\Lambda_b} - 3M_\Lambda\right) + \mathrm{Re}\,F_2G_2^*\left(q^2 + 4p_\Lambda \cdot q\right)\right]\,,
\end{aligned} \tag{16}$$

$$\begin{aligned}
I_3 &= 2\,\mathrm{Re}\,F_1G_1^* M_{\Lambda_b}\left(q^2 + 2p_{\Lambda_b} \cdot q\right)\sqrt{E_\Lambda^2 - M_\Lambda^2} - 2M_{\Lambda_b} q^2\sqrt{E_\Lambda^2 - M_\Lambda^2}\,\times \\
&\quad \left[\mathrm{Re}\,F_2G_1^*\left(M_\Lambda + 3M_{\Lambda_b}\right) + \mathrm{Re}\,F_1G_2^*\left(M_\Lambda - 3M_{\Lambda_b}\right) - \mathrm{Re}\,F_2G_2^*\left(q^2 - 4p_{\Lambda_b} \cdot q\right)\right]\,,
\end{aligned} \tag{17}$$

$$\begin{aligned}
I_4 &= \left(|F_1|^2 - |G_1|^2\right)\left[\frac{M_{\Lambda_b}}{M_\Lambda}\left(E_\Lambda^2 - M_\Lambda^2\right)\left(2M_\Lambda^2 - q^2 - 2p_\Lambda \cdot q\right)\right. \\
&\quad \left. - \frac{E_\Lambda}{M_\Lambda}\left(2p_{\Lambda_b} \cdot q\;p_\Lambda \cdot q - q^2 P_{\Lambda_b} \cdot p_\Lambda\right)\right] + \left(|F_2|^2 + |G_2|^2\right) \\
&\quad \times\left[-M_{\Lambda_b} E_\Lambda q^4 + \frac{M_{\Lambda_b}}{M_\Lambda} q^4\left(E_\Lambda^2 - M_\Lambda^2\right)\right] + \left(|F_2|^2 - |G_2|^2\right)
\end{aligned}$$

$$\begin{aligned}
& \times \left[\frac{E_\Lambda}{M_\Lambda} p_{\Lambda_b} \cdot p_\Lambda q^4 + 4M_{\Lambda_b}^2 \left(E_\Lambda^2 - M_\Lambda^2\right) q^2\right] + 2\left(\mathrm{Re}\,F_2F_1^* + \mathrm{Re}\,G_2G_1^*\right) \\
& \times \left[-\frac{M_{\Lambda_b}}{M_\Lambda} E_\Lambda q^2 p_\Lambda \cdot q + \frac{M_{\Lambda_b}^2}{M_\Lambda} q^2 \left(E_\Lambda^2 - M_\Lambda^2\right)\right] + 2\left(\mathrm{Re}\,F_2F_1^* - \mathrm{Re}\,G_2G_1^*\right) \\
& \times \left[E_\Lambda q^2 p_\Lambda \cdot q + M_{\Lambda_b} q^2 \left(E_\Lambda^2 - M_\Lambda^2\right)\right] , \qquad (18) \\
I_5 \;=\; & -\left(|F_1|^2 - |G_1|^2\right)\left(2p_{\Lambda_b} \cdot q \; p_\Lambda \cdot q - q^2 P_{\Lambda_b} \cdot p_\Lambda\right) + \left(|F_2|^2 - |G_2|^2\right) q^4 P_{\Lambda_b} \cdot p_\Lambda \\
& -\left(|F_2|^2 + |G_2|^2\right) M_{\Lambda_b} M_\Lambda q^4 + 2\left(\mathrm{Re}\,F_2F_1^* - \mathrm{Re}\,G_2G_1^*\right) M_\Lambda q^2 p_{\Lambda_b} \cdot q \\
& -2\left(\mathrm{Re}\,F_2F_1^* + \mathrm{Re}\,G_2G_1^*\right) M_{\Lambda_b} q^2 p_\Lambda \cdot q , \qquad (19) \\
I_6 \;=\; & 2\,\mathrm{Im}\,F_1G_1^* M_{\Lambda_b} \sqrt{E_\Lambda^2 - M_\Lambda^2}\left(q^2 - 2P_{\Lambda_b} \cdot q\right) + 2M_{\Lambda_b} q^2 \sqrt{E_\Lambda^2 - M_\Lambda^2} \\
& \times \left[M_{\Lambda_b}\left(\mathrm{Im}\,F_2G_1^* - \mathrm{Im}\,F_1G_2^*\right) - M_\Lambda\left(\mathrm{Im}\,F_2G_1^* + \mathrm{Im}\,F_1G_2^*\right) + q^2\,\mathrm{Im}\,F_2G_2^*\right] . \qquad (20)
\end{aligned}$$

Here the kinematics and the relationships for the form factors are given as follows:

$$\begin{aligned}
q^2 &= M_{\Lambda_b}^2 + M_\Lambda^2 - 2M_{\Lambda_b} E_\Lambda , \\
p_{\Lambda_b} \cdot p_\Lambda &= M_{\Lambda_b} E_\Lambda , \\
p_{\Lambda_b} \cdot q &= M_{\Lambda_b}^2 - M_{\Lambda_b} E_\Lambda , \\
p_\Lambda \cdot q &= M_{\Lambda_b} E_\Lambda - M_\Lambda^2 , \qquad (21)
\end{aligned}$$

and

$$\begin{aligned}
F_j F_k^* &= f_j f_k \left[\frac{|C_R|^2 + |C_L|^2}{4} + \frac{1}{2}\,\mathrm{Re}\,C_L C_R^*\right] , \\
G_j G_k^* &= g_j g_k \left[\frac{|C_R|^2 + |C_L|^2}{4} - \frac{1}{2}\,\mathrm{Re}\,C_L C_R^*\right] , \\
F_j G_k^* &= f_j g_k \left[\frac{|C_R|^2 - |C_L|^2}{4} + \frac{i}{2}\,\mathrm{Im}\,C_L C_R^*\right] , \\
|F_i|^2 + |G_i|^2 &= \frac{1}{4}\left(f_i^2 + g_i^2\right)\left(|C_R|^2 + |C_L|^2\right) + \frac{1}{2}\left(f_i^2 - g_i^2\right)\mathrm{Re}\,C_L C_R^* , \\
|F_i|^2 - |G_i|^2 &= \frac{1}{4}\left(f_i^2 - g_i^2\right)\left(|C_R|^2 + |C_L|^2\right) + \frac{1}{2}\left(f_i^2 + g_i^2\right)\mathrm{Re}\,C_L C_R^* . \qquad (22)
\end{aligned}$$

From Eq. (13), we can find the decay rate of $\Lambda_b \to \Lambda\nu\bar{\nu}$ by integrating the energy of Λ. The solid angle and the numerical values for the decay branching ratio are shown in the next section. In the standard model, the dominant and subdominant contributions to decay rate in Eq. (13) are the first and last terms in Eq. (15), which are proportional to $(f_1^2 + g_1^2)$ and $(f_1 f_2 + g_1 g_2)$, respectively. Since the form factors of f_2 and g_2 are negative [3], the term relating to $(f_1 f_2 + g_1 g_2)$ gives destructive contribution to the decay rate.

The three components of $\vec{P}_\Lambda$ in Eq. (14), corresponding to the longitudinal, normal and transverse polarization asymmetries of Λ, can be also defined by

$$P_i = \frac{d\Gamma\left(\hat{\xi}_B \cdot \hat{e}_i = 1\right) - d\Gamma\left(\hat{\xi}_B \cdot \hat{e}_i = -1\right)}{d\Gamma\left(\hat{\xi}_B \cdot \hat{e}_i = 1\right) + d\Gamma\left(\hat{\xi}_B \cdot \hat{e}_i = -1\right)} , \quad (i = L, N, T) , \qquad (23)$$

respectively.

When Λ is not polarized, that is $\hat{\xi}_\Lambda = 0$, from Eq. (12) by summing the spin of Λ we obtain

$$d\Gamma = \frac{d\Gamma^0}{2}\Big(1 + \alpha_{\Lambda_b}\hat{\xi}_{\Lambda_b}\cdot\hat{e}_L\Big) \tag{24}$$

with

$$\alpha_{\Lambda_b} = \frac{I_2}{I_1}\,. \tag{25}$$

From the above equation, we may write the polarization of Λ_b as P_{Λ_b} defined by

$$P_{\Lambda_b} \equiv \alpha_{\Lambda_b}\,, \tag{26}$$

when $\hat{\xi}_\Lambda = 0$. For unpolarized Λ_b, *i.e.*, $\hat{\xi}_{\Lambda_b} = 0$, one obtains that

$$\vec{P}_\Lambda = \alpha_\Lambda \hat{e}_L\,, \tag{27}$$

where

$$\alpha_\Lambda = \frac{I_3}{I_1}\,, \tag{28}$$

which implies that the Λ polarization is purely longitudinal. In this case, one has that $P_L = \alpha_\Lambda$ and $P_N = P_T = 0$. We note that, in the standard model, the longitudinal polarization of Λ in Eq. (27) and the polarization of Λ_b in Eq. (26) are independent of the couplings due to the cancellations between $I_{3,2}$ and I_1, respectively. Thus, these polarizations in $\Lambda_b \to \Lambda\nu\bar{\nu}$ are constants and the hadronic form factors are the only theoretical uncertainties.

We note that the transverse component (P_T) of the Λ polarization in Eq. (14) is a T-odd quantity. A nonzero value of P_T could indicate CP violation. In the standard model, since there is no CP violating phase in the CKM elements of $V_{tb}V_{ts}^*$, it cannot induce P_T in the decay of $\Lambda_b \to \Lambda\nu\bar{\nu}$ with polarized initial and final baryons. Clearly, if the transverse Λ polarization is measured in an experiment, it could tell us that there exist new CP violating sources and new types of interactions as well in nature.

4 Numerical Analysis

In this section, we study the numerical values of the decay branching ratio and polarizations of $\Lambda_b \to \Lambda\nu\bar{\nu}$ in the standard model and theories of new physics, respectively.

As mentioned in Sec. I, in general there are four hadronic form factors, f_i and g_i ($i = 1, 2$), for the $\Lambda_b \to \Lambda$ transition. But, under the assumption of HQET, the four, related to $\mathcal{F}_1$ and $\mathcal{F}_2$, becomes two. For simplicity, we take HQET as a good approximation and use the results of Ref. [3] where $\mathcal{F}_1$ and $\mathcal{F}_2$ were calculated by using the QCD sum rule approach. However, in the approach there is a undetermined parameter, so called the Borel parameter (M), introduced for the suppression of the contribution from the higher excited and continuum states. It is found that $1.5\,GeV \leq M \leq 1.9\,GeV$ from the analysis of Ref. [3]. For our numerical calculations, if it is not mentioned further, we take $M = 1.7$ as an input value.

The new physics parameters of δ_L and δ_R can be limited by the decay branching ratio of $B \to X_s \nu\bar{\nu}$, given by [7]

$$\frac{B\left(B\to X_s\nu\bar{\nu}\right)}{B\left(B\to X_c e\bar{\nu}\right)} = \frac{3\alpha_{em}^2}{4\pi\sin^4\theta_w}\frac{\left|V_{ts}\right|^2}{\left|V_{cb}\right|^2}\frac{X^2\left(x_t\right)}{f\left(z\right)}\frac{\eta}{\kappa\left(z\right)}\left(\left|1+\delta_L\right|^2+\left|\delta_R\right|^2\right) \tag{29}$$

where $f(z)$ is the phase-space factor, $\kappa(z)$ is the QCD correction for $B \to X_c e\bar{\nu}$, $z = m_c/m_b$, and η denotes the QCD correction to the matrix element of $b \to s\nu\bar{\nu}$. By taking $B(B \to X_c e\bar{\nu}) = 11\%$, $f(z) = 0.49$, $\kappa(z) = 0.88$, $\eta = 0.83$ and $m_t(m_t) = 165\ GeV$, and using the limit of $B(B \to X_s\nu\bar{\nu}) < 7.7 \times 10^{-4}$ [8], we obtain the constraint on $\delta_{L,R}$ as follows:

$$\left|1+\delta_L\right|^2+\left|\delta_R\right|^2 < 19.3\,. \tag{30}$$

Clearly, as we can see from Eq. (30), large ranges for the values of $\delta_{L,R}$ are allowed. However, it will be shown in Sec. 4.2 that by requring the longitudinal polarization of Λ being less than one, the parameters of $\delta_{L,R}$ can be further constrained.

4.1 Decay branching ratio

- *In the standard model*

In this subsection, we estimate the decay branching ratio of $\Lambda_b \to \Lambda\nu\bar{\nu}$ in the standard model with and without the assumption of HQET. It is known that so far there is no full calculation on the form factors of vector and axial vector currents for baryonic decays. Therefore, for the non-HQET case, we still use the results of Ref. [3] but take several values of g_i/f_i $(i = 1, 2)$ around one required by HQET. In Table 1, we show the decay branching ratio with different ratios of g_i/f_i. From the table we clearly see that even the differences of g_i/f_i are up to 20%, the influence on the decay branching ratio is only at a few percent level. Since we know that f_2 $(g_2) \ll f_1$ (g_1) by Eq. (8) due to the suppression of the heavy quark mass, if one excludes the contributions of f_2 and g_2 by taking $g_2 = f_2 = 0$, there will be 15% deviation on the decay branching ratio.

Table 1: Upper table is the branching ratio for $\Lambda_b \to \Lambda\nu\bar{\nu}$ decay with different ratio g_i/f_i; lower one shows the branching ratio while excluding f_2 and g_2.

$g_1/f_1 = g_2/f_2$	0.80	0.90	0.95	1.00	1.10	1.15	1.20
$10^5 B(\Lambda_b \to \Lambda\nu\bar{\nu})$	1.498	1.530	1.547	1.566	1.606	1.627	1.650

g_1/f_1 $(g_2 = f_2 = 0)$	0.80	0.90	0.95	1.00	1.10	1.15	1.20
$10^5 B(\Lambda_b \to \Lambda\nu\bar{\nu})$	1.584	1.684	1.739	1.796	1.920	1.986	2.055

In Figures 1 and 2, we show the differential decay branching ratio as functions of the Λ energy. We note that in Figure 1 there is a turning point around $E_\Lambda \approx 1.9$ GeV. The ratios for $g_i/f_i > 1$ are higher than that of $g_i/f_i \leq 1$ in the higher E_Λ region, whereas it is opposite for the lower one. The reason is due to the second term of $(|F_1|^2 - |G_1|^2)q^2$ in Eq. (15). While lowering E_Λ, q^2 will be increased; and if E_Λ is over 1.9 GeV, because of entering the small q^2 region, the term becomes less important.

Table 2: The branching ratio for the different values of the Borel parameter M.

M	1.5	1.7	1.9
$10^5 B(\Lambda_b \to \Lambda \nu \bar{\nu})$	1.780	1.566	1.554

For completeness, in Table 2 we present the decay branching ratios for different values of the Borel parameter and in Figure 3 we show the differential decay branching ratio with Λ energy. We see that for the smaller Borel parameter there is a larger deviation (14%) comparing with that for $M = 1.7$.

Finally, it is interesting to note that by defining

$$\bar{\alpha}_B = \frac{\int d\Gamma^0 \alpha_B dE_\Lambda}{\int d\Gamma^0 dE_\Lambda}, \quad (B = \Lambda_b, \Lambda)\,, \tag{31}$$

we have that $\bar{\alpha}_\Lambda \approx -1$ and $\bar{\alpha}_{\Lambda_b} \approx -0.33$.

- *New Physics*

If the hadronic sector involves only the left-handed interactions, from Eqs. (15) and (22) we see that the decay rate depends on $|C_L|^2$. However, if the right-handed current interaction is included, the dependence becomes $(|C_R|^2 + |C_L|^2 + Re\ C_L C_R^*)$. Since the interference term is associated with a large product of form factors, $f_1 g_1$, even for a small C_R case, the physics beyond the standard model still makes a sizable effect. In Table 3, we take a few allowed sets of (δ_L, δ_R) from new physics and show the decay branching ratio of $\Lambda_b \to \Lambda \nu \bar{\nu}$.

Table 3: The branching ratio from new physics for the different parameters of δ_L and δ_R with $g_i/f_i = 1$.

$(\delta_L,\ \delta_R)$	$(-2.25, -0.50)$	$(-1.25, -1.50)$	$(0.10, 0.25)$	$(0.50, 2.25)$
$10^5 B(\Lambda_b \to \Lambda \nu \bar{\nu})$	4.32	4.51	2.65	19.5

4.2 Polarization asymmetries

To discuss the numerical values of the Λ polarizations we assume that $I_2/I_1 \hat{e}_L \cdot \hat{\xi}_{\Lambda_b}$ is small so that we shall neglect this term in our calculations. We also assume that $\hat{\xi}_\Lambda = 0$ when we study the Λ_b polarization. For the form factors of f_i and g_i, we will use the relations in Eq. (8) and consider the cases with and without f_2 and g_2. To illustrate the numerical values of the polarizations, we define the average polarization asymmetries as

$$\bar{P}_i = \int_{E_{\min}}^{E_{\max}} P_i dE_\Lambda / M_{\Lambda_b}\,, \qquad i = \Lambda_b, L, N, T \tag{32}$$

where $E_{\max} = \left(M_{\Lambda_b}^2 + M_\Lambda^2\right) / (2M_\Lambda)$ and $E_{\min} = M_\Lambda$.

- *In the standard model*

As discussed before, if there exist only left-handed interactions, the coupling dependence for the longitudinal and normal polarization asymmetries will be cancelled between the numerator and denominator. While for the transverse part, since there are no CP violating phase and long distance effect, it is expected to be zero. It is clear that the theoretical uncertainties for the polarizations are from the hadronic transition form factors and the CKM matrix elements.

Table 4: The average polarization of Λ_b and longitudinal and normal polarizations of Λ with and without f_2 and g_2 in the standard model

$10^2\bar{P}_{B_i}$	$10^2\bar{P}_{\Lambda_b}$	$10^2\bar{P}_L$	$10^2\bar{P}_N$
$f_1/g_1 = f_2/g_2 = 1$	-7.40	-31.30	5.42
$f_1/g_1 = 1, f_2 = g_2 = 0$	-8.66	-27.12	0

In Table 4, we show the average longitudinal and normal polarization asymmetries of Λ and the polarization Λ_b with and without f_2 and g_2 in the standard model. From the table, we see that the effects of f_2 and g_2 are between $13-17\%$. In the HQET limit, the dominant term of the Λ normal polarization asymmetry is proportional to $-(f_1f_2+g_1g_2)q^2\,p_\Lambda\cdot q$ and this contribution is negligible when f_2 and g_2 are small.

- *New Physics*

To search for the new physics effects, in Figure 4, we plot the contour diagrams with several fixed values of the decay branching ratio and the longitudinal polarization of Λ. Here we have assumed that there are no phases for $\delta_{L,R}$. We note that $|C_R|>|C_L|$ corresponds to $\alpha_\Lambda>0$, while $|C_R|<|C_L|$ is for $\alpha_\Lambda<0$, since α_Λ is related to $|C_R|^2-|C_L|^2$. The forbidden regions in second and fourth quadrants denote not only $\alpha_\Lambda>1$ but also $I_{2(3)}/I_1>1$. Therefore, we obtain a further constraint on $\delta_{L,R}$ that $(1+\delta_L)$ and δ_R should take the same sign in order to have the condition of $\alpha_\Lambda\leq 1$. When the decay branching ratio and α_Λ in $\Lambda_b\to\Lambda\nu\bar{\nu}$ are measured, we can determine the magnitude of C_L and C_R and the relative sign (same sign) of them but not the individual.

From Eqs. (19) and (22), we see that if the theory involves only the left-handed interaction, *i.e*, $\delta_L\neq 0$ and $\delta_R=0$, P_N is the same as that in the standard model because of the cancellation of the coupling constants. For the case where $\delta_R\neq 0$, the dominant terms for P_N are proportional to $f_1^2C_LC_R^*$ and $f_1f_2(|C_R|^2+|C_L|^2)$. As we know that $f_2<0$, $f_2\ll f_1$ and $C_LC_R^*>0$ from the constraint of $\bar{\alpha}_\Lambda\leq 1$, even with a small value of $|C_R|$, the sign of P_N can be changed from the positive (SM-like model) to negative. If the opposite sign of P_N is measured experimentally, it clearly tells us that there is new physics of the right-handed interaction. In Table 5, to show the new physics affect for the polarization asymmetries of polarized Λ_b and Λ in the di-neutrino decay, we list the average Λ longitudinal and normal and Λ_b polarization asymmetries with the same sets of (δ_L,δ_R) as Table 3. The distributions for the polarizations of Λ_b and Λ with respect to the Λ energy are shown in Figures $5-6$, respectively.

For the transverse polarization asymmetry (P_T) which is related to CP violation, from Eq. (20) we see that it depends on $Im(1+\delta_L)\delta_R^*$. Thus, a non-vanished CP violating phase

Table 5: The average polarization asymmetries for different values of δ_L and δ_R from new physics with $g_i/f_i = 1$.

δ_L	δ_R	$10^2\bar{P}_{\Lambda_b}$	$10^2\bar{P}_L$	$10^2\bar{P}_N$
-2.25	-0.50	-4.91	-14.68	-8.59
-1.25	-1.50	6.81	23.05	-2.84
0.10	0.25	-6.38	-20.67	-4.77
0.50	2.25	2.51	7.11	-11.42

δ_L or δ_R will induce P_T. In Table 6, we just show a few possible sets of δ_L and δ_R, where the blank values denote the exclusion by the condition of the longitudinal polarization to be less than 1. From the table, we see that the CP violating polarization can be large. In Figure 8, we show P_T in terms of the Λ energy.

Table 6: The average transverse polarization asymmetry ($\bar{P}_T$) for CP violating theories with different complex parameters of $\delta_{L,R}$ and $g_i/f_i = 1$.

$10^2\bar{P}_T$	$\delta_R = 0.1 + i0.05$	$\delta_R = 1.5 + i0.5$	$\delta_R = -0.1 - i0.05$	$\delta_R = -1.5 - i1.0$
$\delta_L = 0.1 + i0.05$	1.39	3.22	$--$	$--$
$\delta_L = 0.5 + i0.1$	1.00	3.11	$--$	$--$
$\delta_L = -2.1 + i0.5$	$--$	$--$	2.53	1.50
$\delta_L = -2.5 + i1.5$	$--$	$--$	1.88	16.39

5 Conclusions

We have studied the decay of $\Lambda_b \to \Lambda\nu\bar{\nu}$ with the polarized baryons of Λ_b and Λ. The general form for the decay branching rate and the polarizations of Λ_b and Λ in terms of the general hadronic form factors have been given.

In the standard model, we have found that the decay branching ratio of $\Lambda_b \to \Lambda\nu\bar{\nu}$ is between 1.5 to 2.0×10^{-5}. The average longitudinal polarization of Λ is around 30% while that of the normal one is small. Moreover, since there is no CP violating phase from $V_{tb}V_{ts}^*$, the Λ transverse polarization is expected to be zero. The magnitude of the average Λ_b polarization is below 10%.

With new physics, such as the possible right-handed interaction of $\delta_R = 0.50$, the decay branching ratio can be as large as 4×10^{-5}, and the magnitude of $\bar{P}_L$ and $\bar{P}_{\Lambda_b}$ become smaller while $\bar{P}_N$ gets larger. In the CP violating theories, the CP violating transverse Λ polarization can be up to 16%, which could be accessible in future experiments.

Acknowledgments

This work was supported in part by the National Science Council of the Republic of China under contract numbers NSC-89-2112-M-007-054 and NSC-89-2112-M-006-004.

References

[1] CLEO Collaboration, M. S. Alam et. al., *Phys. Rev. Lett.* **74** (1995) 2885.

[2] N. Cabibbo, *Phys. Rev. Lett.* **10** (1963) 531; M. Kobayashi and T. Maskawa, *Prog. Theor. Phys.* **49** (1973) 652.

[3] Chao-Shang Huang and Hua-Gang Yan, *Phys Rev.* **D59** (1999) 114022.

[4] T.M. Aliev and M. Savci, *J. Phys.* **G26** (2000) 997.

[5] D. Rein and L. M. Sehgal, *Phys. Rev.* **D39** (1989) 3325; J. Hagelin and L. S. Littenberg, *Prog. Part. Nucl. Phys.* **23** (1989) 1; M. Lu and M. B. Wise, *Phys. Lett.* **B324** (1994) 461; C. Q. Geng, I. J. Hsu, and Y. C. Lin, *Phys. Lett.* **B355** (1995) 569; C. Q. Geng, I. J. Hsu, and C. W. Wang, *Prog. Theor. Phys.* **101** (1999) 937.

[6] G. Buchalla and A.J. Buras, *Nucl. Phys.* **B412** (1994) 106.

[7] G. Buchalla, A. J. Buras and M. E. Lautenbacher, **Rev. Mod. Phys. 68** (1996) 1230.

[8] ALEPH Collaboration, P. Perrodo *et al.,* in ICHEP '96, Proceedings of the 28th International Conference on High Energy Physics, Warsaw, Poland, edited by Z. Ajduk and A. Wroblewski (World Scientific, Singapore, 1997).

[9] T. Mannel, W. Roberts and Z. Ryzak *Nucl. Phys.* **B355** (1991) 38.

[10] T. Mannel and S. Recksiegel, *J. Phys.* **G24** (1998) 979.

Figure Captions

Figure 1: The differential decay branching ratio as a function of Λ energy with different values of g_i/f_i $(i = 1, 2)$. The solid curve denotes $g_i/f_i = 1$. The thick dashed, dash-dotted, and dotted curves stand for $g_i/f_i = 1.10$, 1.15, and 1.20, while the thin ones for $g_i/f_i = 0.95$, 0.90, and 0.80, respectively.

Figure 2: The differential decay branching ratio as a function of Λ energy with $f_2 = g_2 = 0$ and different values g_1/f_1. The legend of g_1/f_1 is the same as Figure 1.

Figure 3: The differential decay branching ratio as a function of Λ energy with different values of the Borel parameter: $M = 1.5$ (dashed line), $M = 1.7$ (solid line), $M = 1.9$ (dot dashed line).

Figure 4: The elliptic closed curves represent the decay branching ratios from inside in turn as (1.0, 1.3, 1.6, 2.5, 3.0) $\times 10^{-5}$. The lines in first and third quadrants correspond to $P_L = \alpha_\Lambda$ being ±1.0, ±0.8, ±0.5, and ±0.3, respectively.

Figure 5: The distribution of P_{Λ_b} as a function of E_Λ/M_{Λ_b} with various new physics parameters of (δ_L, δ_R), where the solid, dotted, dashed, dense-dotted, and dash-dotted curves correspond to $(\delta_L, 0)$, $(0.10, 0.25)$, $(-2.25. -0.50)$, $(0.50, 2.25)$, and $(-1.25, -1.50)$, respectively, and δ_L expresses arbitrary value.

Figure 6: The distribution of P_L as a function of E_Λ/M_{Λ_b}. Legend is the same as Figure 5.

Figure 7: The distribution of P_N as a function of E_Λ/M_{Λ_b}. Legend is the same as Figure 5.

Figure 8: The distribution of P_T as a function of E_Λ/M_{Λ_b} with various new physics parameters of (δ_L, δ_R), where the solid, dotted, dashed, and dash-dotted curves correspond to $(-2.1 + 0.5i, -0.1 - 0.05i)$, $(-2.5 + 1.5i, -1.5 - i)$, $(-2.1 + 0.5i, -1.5 - i)$, and $(-2.5 + 1.5i, -0.1 - 0.05i)$, respectively.

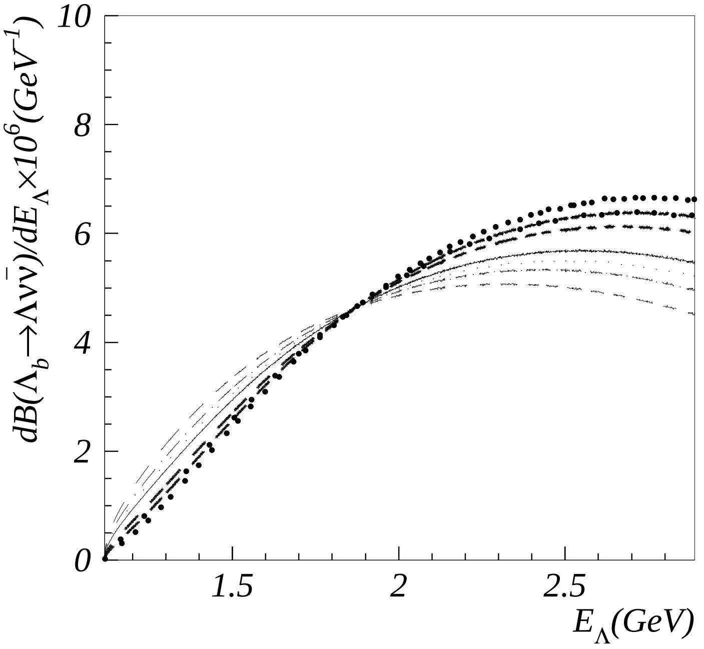

Figure 1: The differential decay branching ratio as a function of Λ energy with different values of g_i/f_i $(i = 1, 2)$. The solid curve denotes $g_i/f_i = 1$. The thick dashed, dash-dotted, and dotted curves stand for $g_i/f_i = 1.10$, 1.15, and 1.20, while the thin ones for $g_i/f_i = 0.95$, 0.90, and 0.80, respectively.

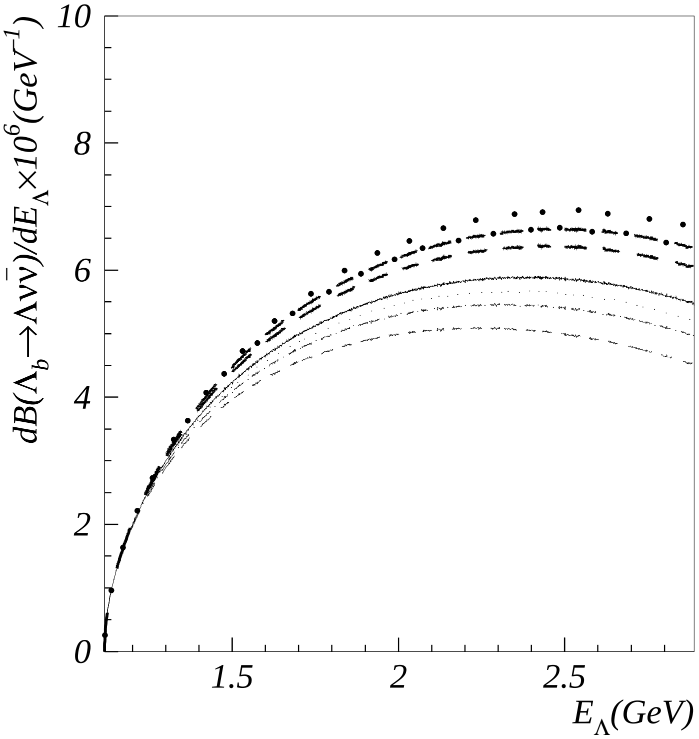

Figure 2: The differential decay branching ratio as a function of Λ energy with $f_2 = g_2 = 0$ and different values g_1/f_1. The legend of g_1/f_1 is the same as Figure 1.

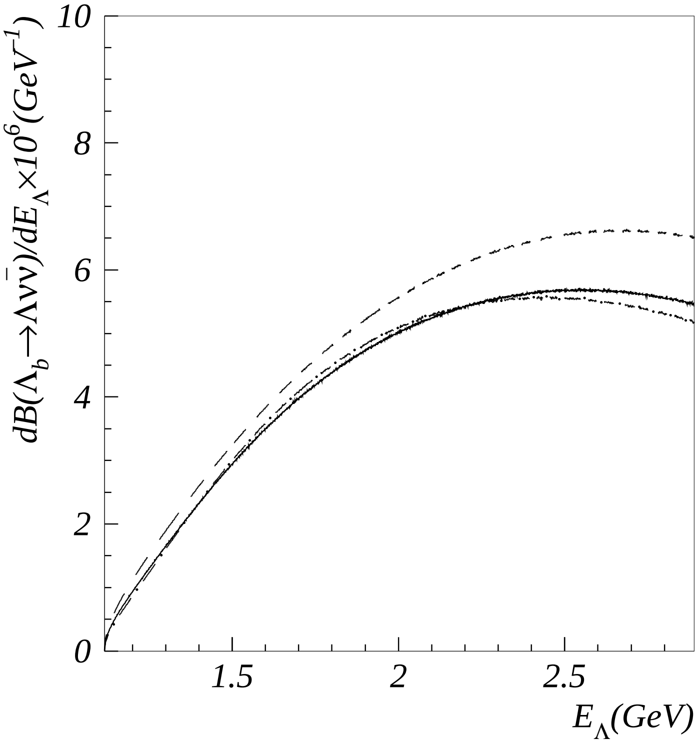

Figure 3: The differential decay branching ratio as a function of Λ energy with different values of the Borel parameter: $M = 1.5$ (dashed line), $M = 1.7$ (solid line), $M = 1.9$ (dot dashed line).

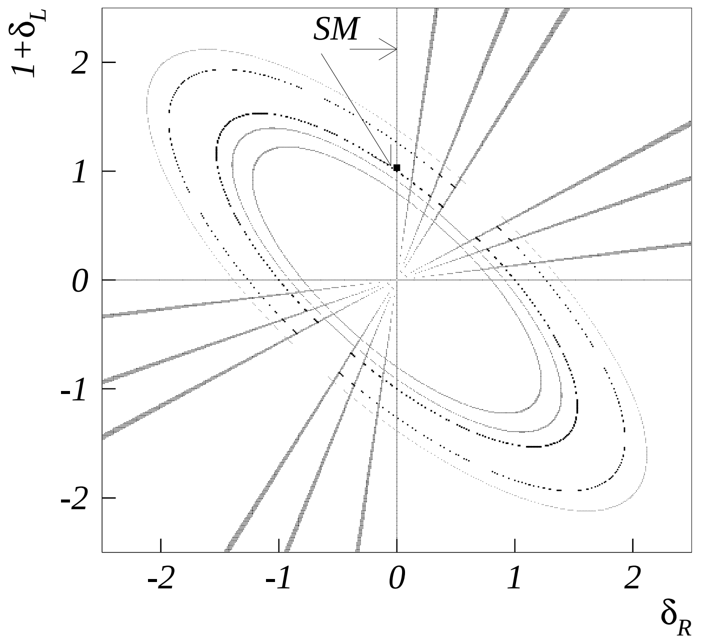

Figure 4: The elliptic closed curves represent the decay branching ratios from inside in turn as (1.0, 1.3, 1.6, 2.5, 3.0) $\times 10^{-5}$. The lines in first and third quadrants correspond to $P_L = \alpha_\Lambda$ being ±1.0, ±0.8, ±0.5, and ±0.3, respectively.

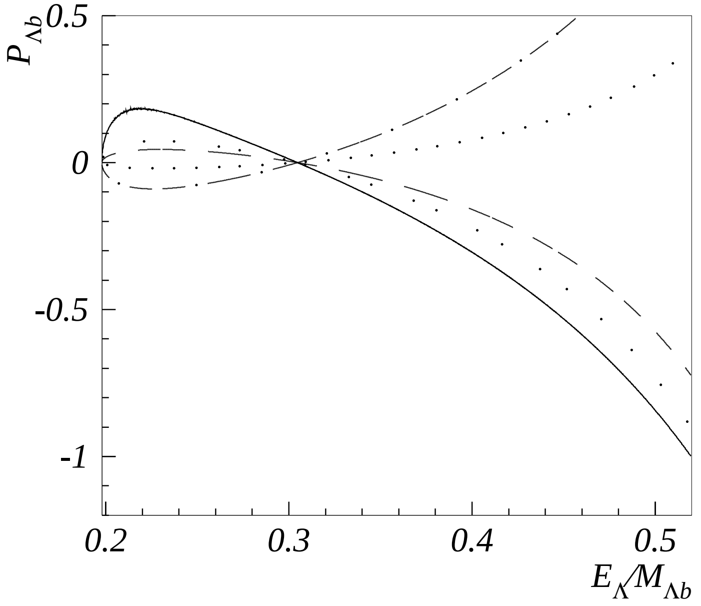

Figure 5: The distribution of P_{Λ_b} as a function of E_Λ/M_{Λ_b} with various new physics parameters of (δ_L, δ_R), where the solid, dotted, dashed, dense-dotted, and dash-dotted curves correspond to $(\delta_L, 0)$, $(0.10, 0.25)$, $(-2.25. -0.50)$, $(0.50, 2.25)$, and $(-1.25, -1.50)$, respectively, and δ_L expresses arbitrary value.

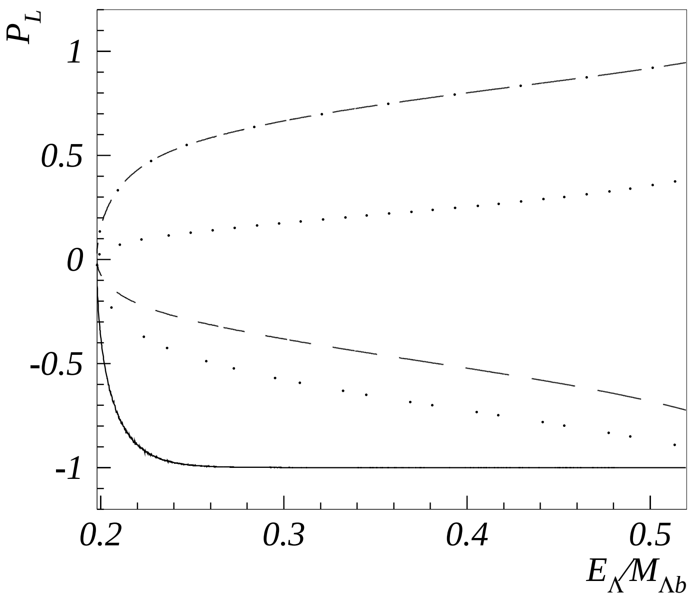

Figure 6: The distribution of P_L as a function of E_Λ/M_{Λ_b}. Legend is the same as Figure 5.

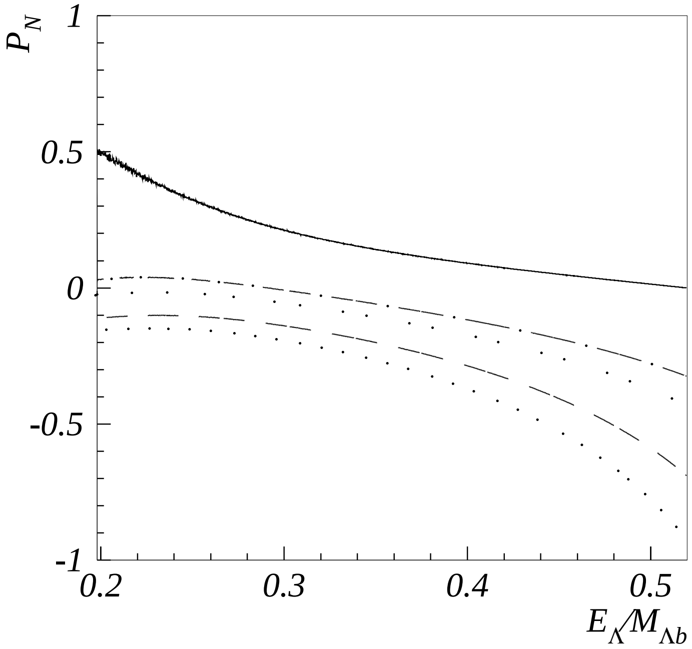

Figure 7: The distribution of P_N as a function of E_Λ/M_{Λ_b}. Legend is the same as Figure 5.

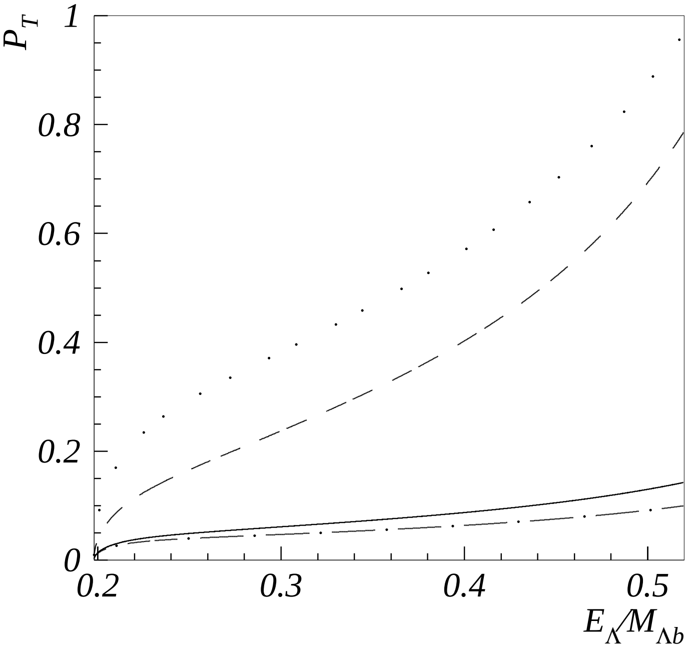

Figure 8: The distribution of P_T as a function of E_Λ/M_{Λ_b} with various new physics parameters of (δ_L, δ_R), where the solid, dotted, dashed, and dash-dotted curves correspond to $(-2.1+0.5i, -0.1-0.05i)$, $(-2.5+1.5i, -1.5-i)$, $(-2.1+0.5i, -1.5-i)$, and $(-2.5+1.5i, -0.1-0.05i)$, respectively.